Digital Signal Processing 67 (2017) 131–138

Contents lists available at ScienceDirect

Digital Signal Processing

www.elsevier.com/locate/dsp

Knowledge-aided adaptive detection in partially homogeneous clutter: Joint exploitation of persymmetry and symmetric spectrum

Goffredo Foglia [a], Chengpeng Hao [b,*], Gaetano Giunta [c], Danilo Orlando [d]

[a] ELETTRONICA S.p.A., Via Tiburtina Valeria, 00131 Rome, Italy
[b] Institute of Acoustics, Chinese Academy of Sciences, Beijing 100190, China
[c] University of "Roma TRE", Via Vito Volterra 62, 00146 Rome, Italy
[d] Università degli Studi "Niccolò Cusano", Via Don Carlo Gnocchi 3, 00166 Rome, Italy

ARTICLE INFO

Article history:
Available online 4 May 2017

Keywords:
Adaptive detection
Generalized likelihood ratio test
Partially homogeneous environment
Persymmetry
Symmetric spectrum

ABSTRACT

In this paper, we address the problem of detecting a point-like target embedded in clutter characterized by a symmetrically structured power spectral density and persymmetric covariance matrix. In particular, we consider the so-called partially homogeneous environment, where the cell under test and the training samples share the same covariance matrix up to an unknown power scaling factor. At the design stage, we jointly exploit the spectral properties of the clutter and the persymmetric structure of the clutter covariance matrix to reformulate the decision problem in terms of real variables with an increased number of training samples. Then, we derive two adaptive detectors relying on the Rao test and a suitable modification of the generalized likelihood ratio test (GLRT). The performance analysis, conducted on both simulated and real radar data, confirms the superiority of the newly proposed receivers over the traditional state-of-the-art counterparts which ignore either the persymmetry or the symmetric spectrum.

1. Introduction

In last decades, the problem of detecting a signal vector known up to a scaling factor in the presence of zero-mean, multivariate Gaussian interference with unknown covariance matrix, has received increasing attention in radar community [1]. Starting from the lack of a uniformly most powerful test for the quoted problem, a considerable amount of work has been made to devise adaptive detection schemes. In particular, in [2] Kelly devises and assesses the generalized likelihood ratio test (GLRT) which interestingly ensures the constant false alarm rate (CFAR) property with respect to the disturbance covariance matrix. In [3], another CFAR receiver, the adaptive matched filter (AMF) is proposed resorting to the two-step GLRT design procedure. Compared with Kelly's GLRT, the AMF is less time consuming and may achieve comparable detection performances. More recently, other design criteria have been investigated as an alternative to the GLRT. For instance, in [4] a novel derivation of the AMF is proposed by resorting to the Wald test design criterion, and in [5] the Rao test is used to derive a detector that exhibits enhanced rejection capabilities to mismatched signals [6,7]. Further recent solutions can be found in [8–10].

All the aforementioned solutions assume a homogeneous environment, wherein the training samples (secondary data) are free of signal components and share the same covariance matrix of the clutter as the cell under test (primary data). As a matter of fact, these solutions require the estimate of the clutter covariance matrix (CCM), performed through a sample covariance matrix (SCM), resorting to the secondary data collected from range gates spatially close to the primary data. For the sake of ensuring a performance within 3 dB from the optimum bound, it is well known that $K \geq 2N$ independent and identically distributed (IID) secondary data are required [11,12], where N denotes the data vector size. Unfortunately, a large number of secondary data are not available in practice. This is commonly caused by the presence of power variations over range, clutter discretes, and other outliers [13], which make secondary data no longer representative of the disturbance in primary data. As a consequence, the receivers that use the SCM based on secondary data exhibit significant performance degradations and the CFAR property is no longer ensured [14].

An efficient way to circumvent the lack of a sufficient number of homogeneous secondary data is to exploit some *a priori* information about the scene illuminated by the radar, as it has been found that the adaptive detection can significantly be improved by exploiting the cognitive knowledge-based processing [15–20]. Alternatively, there are two important kinds of *a priori* information

* Corresponding author. Fax: +86 010 8254 7706.
E-mail address: haochengp@mail.ioa.ac.cn (C. Hao).

http://dx.doi.org/10.1016/j.dsp.2017.04.003
1051-2004/

on the clutter which can be incorporated in solving the detection problem in sample-starved scenarios. The first one is the persymmetric structure of the CCM, which comes from the array geometry and means that the CCM is persymmetric about its cross diagonal [21]. The second one is the symmetry in the clutter spectral characteristics, which originates from the properties of the power spectral density and implies that clutter autocorrelation function is real-valued and even [22]. The two kinds of a priori information can yield structures that involve less unknown parameters to characterize the unknown covariance matrix and, hence, allow to obtain an enhanced estimate of the unknown parameters. Many approaches, relying on either the persymmetry or the symmetric spectrum, have been developed to achieve improved detection performances in training-limited scenarios; just to give an example, see [23–35]. More recently, in [36] the authors move one step further towards the design of adaptive detectors that simultaneously exploit the two kinds of a priori information on the clutter.

In this work, we extend the framework proposed in [36] to the design of architectures for partially homogeneous environment (PHE) [37–41], where the primary and secondary data share the same covariance matrix up to an unknown power scaling factor. The consideration about the PHE model is mainly due to variations in terrain as well as the use of guard cells in radar implementation. At the design stage, we jointly exploit the spectral properties of the clutter and the persymmetric structure of the CCM to reformulate the decision problem in terms of real variables with an increased number of secondary data. Then, we derive the Rao test and a two-step modification of the GLRT. The performance investigation, carried out on simulated dataset and real dataset, shows that the joint exploitation of persymmetry and symmetric clutter spectrum can enhance the detection performances. Finally, it deserves emphasizing that the new detectors can work when $K \geq N/4$ instead of $K \geq N$ required by conventional adaptive detectors, where K stands for the length of the secondary data, and N denotes the number of spatial and/or temporal channels.

The remainder of the paper is organized as follows. Section 2 deals with problem formulation, while Section 3 contains receiver derivations. Section 4 provides numerical examples and comparisons. Finally, some concluding remarks and hints for future work are given in Section 4.

Notation

In the sequel, vectors and matrices are denoted by boldface lower-case and upper-case letters, respectively. Symbols $\det(\cdot)$ and $\mathrm{Tr}(\cdot)$ denote the determinant and the trace of a square matrix, respectively. If A and B are scalars, then $A \times B$ is the usual product of scalars; on the other hand, if A and B are generic sets, $A \times B$ denotes the Cartesian product of sets. The imaginary unit is j, i.e., $\sqrt{-1} = j$. The (i,k)-entry of a generic matrix $\boldsymbol{A}$ is denoted by $\{\boldsymbol{A}\}_{i,k}$. Symbols $\boldsymbol{I}_N$ and $\boldsymbol{0}_{N,M}$ represent the $(N \times N)$-dimensional identity matrix, and the $(N \times M)$ matrix of zeros, respectively. As to the numerical sets, $\mathbb{R}$ is the set of real numbers, $\mathbb{R}^{N\times M}$ is the set of $(N \times M)$-dimensional real matrices (or vectors if $M = 1$), $\mathbb{C}$ is the set of complex numbers, and $\mathbb{C}^{N\times M}$ is the set of $(N \times M)$-dimensional complex matrices (or vectors if $M = 1$). The real and imaginary parts of a complex vector or scalar are denoted by $\Re(\cdot)$ and $\Im(\cdot)$, respectively. Symbol $\boldsymbol{S}_{++}$ is used to represent the set of $N \times N$ positive definite symmetric matrices. Symbols $(\cdot)^T$, $(\cdot)^\dagger$, and $\ln(\cdot)$ stand for transpose, conjugate transpose, and natural logarithm, respectively. Finally, symbol $E[\cdot]$ denotes statistical expectation, and $X \propto Y$ means that X is proportional to Y.

2. Problem formulation

In this section, we introduce the detection problem at hand and show that, under the assumption of a persymmetric structure of the CCM, it is equivalent to another decision problem dealing with independent circularly symmetric complex vectors. Then, we reformulate the latter decision problem exploiting the symmetric spectrum for the clutter, which allows us to transfer the data from the complex to the real domain.

To this end, let us begin by formulating the initial problem in terms of a binary hypothesis test. Specifically, we assume that the considered sensing systems acquires data from $N \geq 2$ channels which can be spatial and/or temporal. The echoes from the cell under test are properly pre-processed, namely, the received signals are downconverted to baseband or an intermediate frequency; then, they are sampled and organized to form an N-dimensional vector, $\boldsymbol{r}_0$ say. We want to test whether or not $\boldsymbol{r}_0$ contains useful target echoes assuming the presence of a set of K secondary data. Summarizing, we can write this decision problem as follows

$$\begin{cases} H_0 : \begin{cases} \boldsymbol{r}_0 = \boldsymbol{n}_0, \\ \boldsymbol{r}_{0k} = \boldsymbol{n}_{0k}, \qquad k = 1, \ldots, K, \end{cases} \\ H_1 : \begin{cases} \boldsymbol{r}_0 = \alpha \boldsymbol{v} + \boldsymbol{n}_0, \\ \boldsymbol{r}_{0k} = \boldsymbol{n}_{0k}, \qquad k = 1, \ldots, K, \end{cases} \end{cases} \tag{1}$$

where

- $\boldsymbol{v} = \boldsymbol{v}_r + j\boldsymbol{v}_i \in \mathbb{C}^{N\times 1}$ with $\|\boldsymbol{v}\| = 1$, $\boldsymbol{v}_r = \Re\{\boldsymbol{v}\}$, and $\boldsymbol{v}_i = \Im\{\boldsymbol{v}\}$ is the nominal steering vector;
- $\alpha = \alpha_r + j\alpha_i \in \mathbb{C}$ with $\alpha_r = \Re\{\alpha\}$ and $\alpha_i = \Im\{\alpha\}$ represents the target response which is modeled in terms of an unknown deterministic factor accounting for target reflectivity and channel propagation effects;
- $\boldsymbol{n}_0$, $\boldsymbol{n}_{0k} \in \mathbb{C}^{N\times 1}$, $k = 1, \ldots, K$, are IID complex normal random vectors with zero mean and unknown positive definite covariance matrices given by

$$E\left[\boldsymbol{n}_0\boldsymbol{n}_0^\dagger\right] = \overline{\boldsymbol{M}}, \quad E\left[\boldsymbol{n}_{0k}\boldsymbol{n}_{0k}^\dagger\right] = \gamma\overline{\boldsymbol{M}}, \tag{2}$$

with $\overline{\boldsymbol{M}} \in \boldsymbol{S}_{++}$ and $\gamma > 0$ an unknown power scaling factor.

Observe that for an active system utilizing symmetrically spaced linear array and/or pulsed train, both $\overline{\boldsymbol{M}}$ and $\boldsymbol{v}$ have the persymmetric property. More precisely, $\boldsymbol{v} = \boldsymbol{J}_N\boldsymbol{v}^*$ and $\overline{\boldsymbol{M}}$ belongs to the set $\mathcal{P}$ defined as

$$\overline{\boldsymbol{M}} \in \mathcal{P} \quad \text{iff} \quad \overline{\boldsymbol{M}} = \boldsymbol{J}_N\overline{\boldsymbol{M}}^*\boldsymbol{J}_N, \tag{3}$$

where $\boldsymbol{J}_N \in \mathbb{R}^{N\times N}$ is the permutation matrix with unit anti-diagonal elements and zeros elsewhere, i.e.,

$$\boldsymbol{J}_N = \begin{bmatrix} 0 & 0 & \cdots & 0 & 1 \\ 0 & 0 & \cdots & 1 & 0 \\ \vdots & \iddots & \iddots & \iddots & \vdots \\ 1 & 0 & \cdots & 0 & 0 \end{bmatrix}. \tag{4}$$

Now, following the lead of Appendix B of [24], we can recast problem (1) in terms of

$$\begin{aligned} &\boldsymbol{r}_1 = \frac{\boldsymbol{r}_0 + \boldsymbol{J}_N\boldsymbol{r}_0^*}{2}, \quad \boldsymbol{r}_2 = \frac{\boldsymbol{r}_0 - \boldsymbol{J}_N\boldsymbol{r}_0^*}{2}, \\ &\boldsymbol{r}_{1k} = \frac{\boldsymbol{r}_{0k} + \boldsymbol{J}_N\boldsymbol{r}_{0k}^*}{2}, \ \boldsymbol{r}_{2k} = \frac{\boldsymbol{r}_{0k} - \boldsymbol{J}_N\boldsymbol{r}_{0k}^*}{2}, \ k = 1, \ldots, K, \end{aligned} \tag{5}$$

which are independent circularly symmetric complex Gaussian vectors with means depending on which hypothesis is in force and covariance matrix given by

$$E\left[\boldsymbol{r}_1\boldsymbol{r}_1^\dagger\right] = \overline{\boldsymbol{M}}/2, \quad E\left[\boldsymbol{r}_{1k}\boldsymbol{r}_{1k}^\dagger\right] = \gamma\overline{\boldsymbol{M}}/2. \tag{6}$$

Thus, we can write

$$\begin{cases} H_0: \begin{cases} \boldsymbol{r}_1 = \boldsymbol{n}_1,\ \boldsymbol{r}_2 = \boldsymbol{n}_2, \\ \boldsymbol{r}_{1k} = \boldsymbol{n}_{1k},\ \boldsymbol{r}_{2k} = \boldsymbol{n}_{2k}, \qquad k = 1, \ldots, K, \end{cases} \\ H_1: \begin{cases} \boldsymbol{r}_1 = \alpha_r \boldsymbol{v} + \boldsymbol{n}_1, \boldsymbol{r}_2 = \alpha_i \boldsymbol{v} + \boldsymbol{n}_2 \\ \boldsymbol{r}_{1k} = \boldsymbol{n}_{1k},\ \boldsymbol{r}_{2k} = \boldsymbol{n}_{2k}, \qquad k = 1, \ldots, K, \end{cases} \end{cases} \tag{7}$$

where

$$\boldsymbol{n}_1 = \frac{\boldsymbol{n}_0 + \boldsymbol{J}_N \boldsymbol{n}_0^*}{2},\ \boldsymbol{n}_2 = \frac{\boldsymbol{n}_0 - \boldsymbol{J}_N \boldsymbol{n}_0^*}{2},$$
$$\boldsymbol{n}_{1k} = \frac{\boldsymbol{n}_{0k} + \boldsymbol{J}_N \boldsymbol{n}_{0k}^*}{2},\ \boldsymbol{n}_{2k} = \frac{\boldsymbol{n}_{0k} - \boldsymbol{J}_N \boldsymbol{n}_{0k}^*}{2}. \tag{8}$$

Problem (7) can be further recast exploiting the fact that clutter spectrum is real and even. Otherwise stated, the CCM is real and, hence, it is possible to express problem (7) in terms of the following quantities

$$\begin{aligned} &\boldsymbol{z}_{1r} = \Re(\boldsymbol{r}_1),\ \boldsymbol{z}_{1i} = \Im(\boldsymbol{r}_1), \boldsymbol{z}_{2r} = \Re(\boldsymbol{r}_2), \boldsymbol{z}_{2i} = \Im(\boldsymbol{r}_2), \\ &\boldsymbol{z}_{1kr} = \Re(\boldsymbol{r}_{1k}),\ \boldsymbol{z}_{1ki} = \Im(\boldsymbol{r}_{1k}), \\ &\boldsymbol{z}_{2kr} = \Re(\boldsymbol{r}_{2k}), \boldsymbol{z}_{2ki} = \Im(\boldsymbol{r}_{2k}),\ k = 1, \ldots, K. \end{aligned} \tag{9}$$

It is easy to know that $\boldsymbol{z}_{1r}$, $\boldsymbol{z}_{1i}$, $\boldsymbol{z}_{2r}$, $\boldsymbol{z}_{2i}$, $\boldsymbol{z}_{1kr}$, $\boldsymbol{z}_{1ki}$, $\boldsymbol{z}_{2kr}$, and $\boldsymbol{z}_{2ki}$ are statistically independent real Gaussian vector with means depending on which hypothesis is in force and covariance matrix given by

$$\begin{aligned} &E\left[\boldsymbol{z}_{1r}\boldsymbol{z}_{1r}^\dagger\right] = E\left[\boldsymbol{z}_{1i}\boldsymbol{z}_{1i}^\dagger\right] = E\left[\boldsymbol{z}_{2r}\boldsymbol{z}_{2r}^\dagger\right] = E\left[\boldsymbol{z}_{2i}\boldsymbol{z}_{2i}^\dagger\right] = \boldsymbol{M}, \\ &E\left[\boldsymbol{z}_{1kr}\boldsymbol{z}_{1kr}^\dagger\right] = E\left[\boldsymbol{z}_{1ki}\boldsymbol{z}_{1ki}^\dagger\right] = E\left[\boldsymbol{z}_{2kr}\boldsymbol{z}_{2kr}^\dagger\right] = E\left[\boldsymbol{z}_{2ki}\boldsymbol{z}_{2ki}^\dagger\right] = \gamma\boldsymbol{M} \end{aligned} \tag{10}$$

with $\boldsymbol{M} = \frac{1}{4}\overline{\boldsymbol{M}} \in \mathbb{R}^{N\times N}$. Thus, problem (7) is equivalent to

$$\begin{cases} H_0: \begin{cases} \boldsymbol{z}_{1r} = \boldsymbol{n}_{1r},\ \boldsymbol{z}_{1i} = \boldsymbol{n}_{1i},\ \boldsymbol{z}_{2r} = \boldsymbol{n}_{2r},\ \boldsymbol{z}_{2i} = \boldsymbol{n}_{2i}, \\ \boldsymbol{z}_{1kr} = \boldsymbol{n}_{1kr},\ \boldsymbol{r}_{1ki} = \boldsymbol{n}_{1ki}, \\ \boldsymbol{z}_{2kr} = \boldsymbol{n}_{2kr},\ \boldsymbol{r}_{2ki} = \boldsymbol{n}_{2ki},\ k = 1, \ldots, K, \end{cases} \\ H_1: \begin{cases} \boldsymbol{z}_{1r} = \alpha_r \boldsymbol{v}_r + \boldsymbol{n}_{1r},\ \boldsymbol{z}_{1i} = \alpha_r \boldsymbol{v}_i + \boldsymbol{n}_{1i}, \\ \boldsymbol{z}_{2r} = \alpha_i \boldsymbol{v}_r + \boldsymbol{n}_{2r}, \boldsymbol{z}_{2i} = \alpha_i \boldsymbol{v}_i + \boldsymbol{n}_{2i}, \\ \boldsymbol{z}_{1kr} = \boldsymbol{n}_{1kr},\ \boldsymbol{z}_{1ki} = \boldsymbol{n}_{1ki}, \\ \boldsymbol{z}_{2kr} = \boldsymbol{n}_{2kr},\ \boldsymbol{z}_{2ki} = \boldsymbol{n}_{2ki},\ k = 1, \ldots, K, \end{cases} \end{cases} \tag{11}$$

where

$$\begin{aligned} &\boldsymbol{n}_{1r} = \Re(\boldsymbol{n}_1),\ \boldsymbol{n}_{1i} = \Im(\boldsymbol{n}_1), \boldsymbol{n}_{2r} = \Re(\boldsymbol{n}_2), \boldsymbol{n}_{2i} = \Im(\boldsymbol{n}_2), \\ &\boldsymbol{n}_{1kr} = \Re(\boldsymbol{n}_{1k}),\ \boldsymbol{n}_{1ki} = \Im(\boldsymbol{n}_{1k}), \\ &\boldsymbol{n}_{2kr} = \Re(\boldsymbol{n}_{2k}), \boldsymbol{n}_{2ki} = \Im(\boldsymbol{n}_{2k}),\ k = 1, \ldots, K. \end{aligned} \tag{12}$$

Remark 1. Comparison of (1) and (11) indicates that transferring problem (1) to problem (11) is equivalent to multiply the number of secondary data by four and, hence, the new receivers obtained by solving problem (7) would work under the constraint $4K \geq N$ instead of $K \geq N$ which is required by the traditional detectors in [2–5]. Moreover, as shown in Section 4, the new receivers exhibit superior detection performance with respect to the receivers which exploit either the persymmetric structure of the CCM or the symmetric spectrum for the clutter.

3. Detector designs

Since no uniformly most powerful test exists for problem (11), we seek decision statistics which achieve higher detection probability with reasonable computational complexity and ensure the CFAR property [42]. Observe also that the mathematical derivation of the plain GLRT and the Wald test for the problem at hand is a formidable task (at least to the best of authors' knowledge). For above reasons, we resort to the Rao test and a two-step modification of the GLRT to devise two adaptive architectures.

As a preliminary step toward the derivation of the receivers, let us denote by following quantities.

- $\boldsymbol{Z} = [\boldsymbol{Z}_1\ \boldsymbol{Z}_2] \in \mathbb{R}^{N\times 4}$ denotes the primary data matrix with $\boldsymbol{Z}_1 = [\boldsymbol{z}_{1r}\ \boldsymbol{z}_{1i}] \in \mathbb{R}^{N\times 2}$ and $\boldsymbol{Z}_2 = [\boldsymbol{z}_{2r}\ \boldsymbol{z}_{2i}] \in \mathbb{R}^{N\times 2}$.
- $\boldsymbol{Z}_K = [\boldsymbol{Z}_{1K}\ \boldsymbol{Z}_{2K}] \in \mathbb{R}^{N\times 4K}$ denotes the secondary data matrix with $\boldsymbol{Z}_{1K} = [\boldsymbol{z}_{11r} \ldots \boldsymbol{z}_{1Kr}\ \boldsymbol{z}_{11i} \ldots \boldsymbol{z}_{1Ki}] \in \mathbb{R}^{N\times 2K}$ and $\boldsymbol{Z}_{2K} = [\boldsymbol{z}_{21r} \ldots \boldsymbol{z}_{2Kr}\ \boldsymbol{z}_{21i} \ldots \boldsymbol{z}_{2Ki}] \in \mathbb{R}^{N\times 2K}$.
- $\boldsymbol{V} = [\boldsymbol{v}_r\ \boldsymbol{v}_i] \in \mathbb{R}^{N\times 2}$ denotes the nominal steering matrix.
- $\boldsymbol{\theta}_A = [\alpha_r, \alpha_i]^T \in \mathbb{R}^{2\times 1}$ denotes the signal parameter vector.
- $\boldsymbol{\theta}_B = \left[\gamma\ \boldsymbol{f}^T(\boldsymbol{M})\right]^T \in \mathbb{R}^{(N-1)N/2+1\times 1}$ denotes the nuisance parameter vector, where $\boldsymbol{f}(\cdot)$ is a vector-valued function that selects in unequivocal way (bijection) the elements of a symmetric matrix. Observe that since $\boldsymbol{M} \in \boldsymbol{S}_{++}$, it can be well represented by the $[(N-1)N/2]$-dimensional vector.
- $\boldsymbol{\theta} = \left[\boldsymbol{\theta}_A^T\ \boldsymbol{\theta}_B^T\right]^T$ contains all unknown parameters, and $\widehat{\boldsymbol{\theta}}_0 = \left[\boldsymbol{\theta}_{A0}^T\ \widehat{\boldsymbol{\theta}}_{B0}^T\right]^T$ denotes the maximum likelihood estimate (MLE) of $\boldsymbol{\theta}$ under H_0 with $\boldsymbol{\theta}_{A0} = [0\ 0]^T$. Note that $\widehat{\boldsymbol{\theta}}_{B0}$ is the MLE of $\boldsymbol{\theta}_B$ under H_0.

Under the above assumption, the joint probability density function (PDF) of $\boldsymbol{Z}$ and $\boldsymbol{Z}_K$ under H_l, $l = 0, 1$, is given by

$$f(\boldsymbol{Z}, \boldsymbol{Z}_K; \boldsymbol{\theta}, H_l) = \frac{\gamma^{-2NK}}{(2\pi)^{2N(K+1)} \det^{2(K+1)}(\boldsymbol{M})} \times \exp\left\{-\frac{1}{2}\mathrm{Tr}\left[\boldsymbol{M}^{-1}\boldsymbol{T}_l(l\alpha_r, l\alpha_i)\right]\right\}, \tag{13}$$

where

$$\boldsymbol{T}_l(l\alpha_r, l\alpha_i) = (\boldsymbol{Z}_1 - l\alpha_r\boldsymbol{V})(\boldsymbol{Z}_1 - l\alpha_r\boldsymbol{V})^T + (\boldsymbol{Z}_2 - l\alpha_i\boldsymbol{V})(\boldsymbol{Z}_2 - l\alpha_i\boldsymbol{V})^T + \frac{1}{\gamma}\boldsymbol{S} \tag{14}$$

with $\boldsymbol{S} = \boldsymbol{Z}_K\boldsymbol{Z}_K^T$ the SCM based on secondary data only.

3.1. Rao test

In this subsection, we focus on the Rao test design criterion, which is often simpler than the GLRT and is also asymptotically equivalent to the latter. The binary hypothesis (11) for the problem considered induces the following equivalent parameter hypothesis [43]

$$\begin{cases} H_0: \boldsymbol{\theta}_A = \boldsymbol{\theta}_{A0}, \quad \boldsymbol{\theta}_B, \\ H_1: \boldsymbol{\theta}_A \neq \boldsymbol{\theta}_{A0}, \quad \boldsymbol{\theta}_B. \end{cases} \tag{15}$$

Let $\boldsymbol{J}(\boldsymbol{\theta})$ the Fisher information matrix, which can be partitioned as [43]

$$\boldsymbol{J}(\boldsymbol{\theta}) = -E\left[\frac{\partial^2}{\partial\boldsymbol{\theta}\partial\boldsymbol{\theta}^T}\ln f(\boldsymbol{Z}, \boldsymbol{Z}_K; \boldsymbol{\theta}, H_1)\right] = \begin{bmatrix} \boldsymbol{J}_{AA}(\boldsymbol{\theta}) & \boldsymbol{J}_{AB}(\boldsymbol{\theta}) \\ \boldsymbol{J}_{BA}(\boldsymbol{\theta}) & \boldsymbol{J}_{BB}(\boldsymbol{\theta}) \end{bmatrix}, \tag{16}$$

where

$$\boldsymbol{J}_{PQ}(\boldsymbol{\theta}) = -E\left[\frac{\partial^2}{\partial\boldsymbol{\theta}_X\partial\boldsymbol{\theta}_Y^T}\ln f(\boldsymbol{Z}, \boldsymbol{Z}_K; \boldsymbol{\theta}, H_1)\right] \in \mathbb{R}^{x\times y}. \tag{17}$$

In (17), $(x, y) \in \{A, B\} \times \{A, B\}$,

$$x = \begin{cases} 2, & \text{if } X = A, \\ L, & \text{if } X = B, \end{cases} \tag{18}$$

and

$$y = \begin{cases} 2, & \text{if } Y = A, \\ L, & \text{if } Y = B. \end{cases} \tag{19}$$

Now, we have provided all the definitions to introduce the Rao test, namely

$$\left.\frac{\partial \ln f(\boldsymbol{Z}, \boldsymbol{Z}_K; \boldsymbol{\theta}, H_1)}{\partial \boldsymbol{\theta}_A}\right|^T_{\boldsymbol{\theta}=\widehat{\boldsymbol{\theta}}_0} \left\{\left[\boldsymbol{J}^{-1}(\boldsymbol{\theta})\right]_{AA}\right\}_{\boldsymbol{\theta}=\widehat{\boldsymbol{\theta}}_0} \times \left.\frac{\partial \ln f(\boldsymbol{Z}, \boldsymbol{Z}_K; \boldsymbol{\theta}, H_1)}{\partial \boldsymbol{\theta}_A}\right|_{\boldsymbol{\theta}=\widehat{\boldsymbol{\theta}}_0} \underset{H_0}{\overset{H_1}{\gtrless}} \eta, \tag{20}$$

where η is[1] the threshold value to be set according to the desired P_{fa}, and $\left[\boldsymbol{J}(\boldsymbol{\theta})^{-1}\right]_{AA}$ is the sub-block of the inverse of the Fisher information matrix formed by selecting its first two rows and the first two columns; in addition it can be written as

$$\left[\boldsymbol{J}^{-1}(\boldsymbol{\theta})\right]_{AA} = \left[\boldsymbol{J}_{AA}(\boldsymbol{\theta}) - \boldsymbol{J}_{AB}(\boldsymbol{\theta})\boldsymbol{J}_{BB}^{-1}(\boldsymbol{\theta})\boldsymbol{J}_{BA}(\boldsymbol{\theta})\right]^{-1}. \tag{21}$$

From (20), the derivation of the Rao test is a two-step process. The first one is to obtain the MLE of the nuisance parameters under H_0, and the second one is to evaluate the related terms in (20). Let us begin with the first step. To this end, note that taking the derivative of $\ln f(\boldsymbol{Z}, \boldsymbol{Z}_K; \boldsymbol{\theta}, H_0)$ with respect to $\boldsymbol{M}$ and equating it to zero results in

$$\widehat{\boldsymbol{M}}_0 = \frac{1}{4(K+1)}\left(\frac{1}{\gamma}\boldsymbol{S} + \boldsymbol{Z}\boldsymbol{Z}^T\right). \tag{22}$$

Plugging (22) into (13), we have

$$\begin{aligned} &f(\boldsymbol{Z}, \boldsymbol{Z}_K; \widehat{\boldsymbol{M}}_0, \gamma, H_0) \\ &\propto \left[\gamma^{\frac{NK}{K+1}} \det\left(\frac{1}{\gamma}\boldsymbol{S} + \boldsymbol{Z}\boldsymbol{Z}^T\right)\right]^{-2(K+1)} \\ &= \left[\det(\boldsymbol{S})\gamma^{4-\frac{N}{K+1}} \det\left(\frac{1}{\gamma}\boldsymbol{I}_4 + \boldsymbol{Z}^T\boldsymbol{S}^{-1}\boldsymbol{Z}\right)\right]^{-2(K+1)} \end{aligned} \tag{23}$$

where the last equality comes from

$$\det\left(\frac{1}{\gamma}\boldsymbol{I}_N + \boldsymbol{A}\boldsymbol{B}\right) = \gamma^{4-N}\det\left(\frac{1}{\gamma}\boldsymbol{I}_4 + \boldsymbol{B}\boldsymbol{A}\right) \tag{24}$$

with $\boldsymbol{A} \in \mathbb{R}^{N\times 4}$ and $\boldsymbol{B} \in \mathbb{R}^{4\times N}$ rectangular matrices. Apparently, $\widehat{\gamma}_0$ is obtained by minimizing $\gamma^{4-\frac{N}{K+1}}\det\left(\frac{1}{\gamma}\boldsymbol{I}_4 + \boldsymbol{Z}^T\boldsymbol{S}^{-1}\boldsymbol{Z}\right)$. To this end, we denote by r the rank of $\boldsymbol{S}^{-1/2}\boldsymbol{Z}\boldsymbol{Z}^T\boldsymbol{S}^{-1/2}$; note that $r = \min(N, 4) \geq 2$. Following the lead of Proposition 2 of [44], it is not difficult to show that under the constraint[2] $r > \frac{N}{K+1}$, $\widehat{\gamma}_0$ is the unique positive solution of equation

$$\sum_{i=1}^{r} \frac{\mu_i\gamma}{\mu_i\gamma + 1} = \frac{N}{K+1} \tag{25}$$

with μ_i, $i = 1, \ldots, r$, the non-zero eigenvalues of $\boldsymbol{S}^{-1/2}\boldsymbol{Z}\boldsymbol{Z}^T\boldsymbol{S}^{-1/2}$. Note that (25) can be solved by resorting to the Matlab function '*roots*' which evaluates the eigenvalues of a companion matrix of order $(r+1)\times(r+1)$ at most.

[1] Hereafter, η is used to denote the detection threshold or any proper modification of it for all the considered receivers.

[2] This constraint is looser than $2K \geq N$ which is required to ensure a full-rank estimate of $\boldsymbol{M}$ (see Remark 1) and, hence, it can always be met.

Now, we use the above results to write the test statistic. Specifically, the elements of the first partial derivative of the score function $\ln f(\boldsymbol{Z}, \boldsymbol{Z}_K; \boldsymbol{\theta}, H_1)$ with respect to $\boldsymbol{\theta}_A$ are

$$\begin{aligned} \frac{\partial \ln f(\boldsymbol{Z}, \boldsymbol{Z}_K; \boldsymbol{\theta}, H_1)}{\partial \boldsymbol{\theta}_A} &= \begin{bmatrix} \frac{\partial \ln f(\boldsymbol{Z}, \boldsymbol{Z}_K; \boldsymbol{\theta}, H_1)}{\partial \boldsymbol{\theta}_A}\partial\alpha_r \\ \frac{\partial \ln f(\boldsymbol{Z}, \boldsymbol{Z}_K; \boldsymbol{\theta}, H_1)}{\partial \boldsymbol{\theta}_A}\partial\alpha_i \end{bmatrix} \\ &= 2\begin{bmatrix} \mathrm{Tr}\left[\boldsymbol{V}^T\boldsymbol{M}^{-1}(\boldsymbol{Z}_1 - \alpha_r\boldsymbol{V})\right] \\ \mathrm{Tr}\left[\boldsymbol{V}^T\boldsymbol{M}^{-1}(\boldsymbol{Z}_2 - \alpha_i\boldsymbol{V})\right] \end{bmatrix}. \end{aligned} \tag{26}$$

Thus, we can write

$$\left.\frac{\partial \ln f(\boldsymbol{Z}, \boldsymbol{Z}_K; \boldsymbol{\theta}, H_1)}{\partial \boldsymbol{\theta}_A}\right|_{\boldsymbol{\theta}=\widehat{\boldsymbol{\theta}}_0} = \begin{bmatrix} \mathrm{Tr}\left[\boldsymbol{V}^T\boldsymbol{M}^{-1}\boldsymbol{Z}_1\right] \\ \mathrm{Tr}\left[\boldsymbol{V}^T\boldsymbol{M}^{-1}\boldsymbol{Z}_2\right] \end{bmatrix}. \tag{27}$$

Further developments require evaluating the blocks of the Fisher information matrix. To this end, it can be shown that

$$\boldsymbol{J}_{AA}(\boldsymbol{\theta}) = 2\mathrm{Tr}\left(\boldsymbol{V}^T\boldsymbol{M}^{-1}\boldsymbol{V}\right)\boldsymbol{I}_2. \tag{28}$$

On the other hand, $\boldsymbol{J}_{AB}(\boldsymbol{\theta})$ is a $2\times(L+1)$ matrix whose (l,k)th element is

$$\boldsymbol{J}_{AB}(\boldsymbol{\theta})(l,k) = -E\left[\frac{\partial \ln f(\boldsymbol{Z}, \boldsymbol{Z}_K; \boldsymbol{\theta}, H_1)}{\partial \boldsymbol{\theta}_A(i)\boldsymbol{\theta}_B(j)}\right], \quad l \in (1, \ldots, 2),\ k \in (1, \ldots L), \tag{29}$$

where $\boldsymbol{\theta}_A(t)$ and $\boldsymbol{\theta}_B(t)$ denote the tth element of $\boldsymbol{\theta}_A$ and $\boldsymbol{\theta}_B$, respectively. It is easy to show that $\boldsymbol{J}_{AB}(\boldsymbol{\theta})(l,k)$ is linear function of $\boldsymbol{Z}_1 - \alpha_r\boldsymbol{V}$ and $\boldsymbol{Z}_2 - \alpha_i\boldsymbol{V}$ and, hence, we can conclude that $\boldsymbol{J}_{AB}(\boldsymbol{\theta}) = \boldsymbol{0}_{2,L+1}$, because of $E(\boldsymbol{Z}_1 - \alpha_r\boldsymbol{V}) = E(\boldsymbol{Z}_2 - \alpha_i\boldsymbol{V}) = \boldsymbol{0}_{N,2}$. It follows that

$$\left[\boldsymbol{J}^{-1}(\boldsymbol{\theta})\right]_{AA} = \frac{1}{2\mathrm{Tr}\left(\boldsymbol{V}^T\boldsymbol{M}^{-1}\boldsymbol{V}\right)}\boldsymbol{I}_2. \tag{30}$$

Gathering the above results, the Rao test can be finally given by

$$\frac{\mathrm{Tr}^2\left(\boldsymbol{V}^T\widehat{\boldsymbol{M}}_0^{-1}\boldsymbol{Z}_1\right) + \mathrm{Tr}^2\left(\boldsymbol{V}^T\widehat{\boldsymbol{M}}_0^{-1}\boldsymbol{Z}_2\right)}{\mathrm{Tr}\left(\boldsymbol{V}^T\widehat{\boldsymbol{M}}_0^{-1}\boldsymbol{V}\right)} \underset{H_0}{\overset{H_1}{\gtrless}} \eta, \tag{31}$$

where $\widehat{\boldsymbol{M}}_0$ is given by (22) by using $\widehat{\gamma}_0$ in place of γ. In the sequel, we refer to detector (31) as the persymmetric and symmetric spectrum Rao test for PHE (PSS-RAO-PHE).

3.2. GLRT-based architecture

In this subsection, we derive a detector based on a two-step modification of the GLRT. In order to facilitate the derivations of the test, we move the power scaling factor from the secondary data to primary data. Precisely, we define $\boldsymbol{\Sigma} = \gamma\boldsymbol{M}$, which implies that $\boldsymbol{M} = \lambda\boldsymbol{\Sigma}$ with $\lambda = \frac{1}{\gamma}$, namely,

$$\begin{aligned} &E\left[\boldsymbol{n}_{1r}\boldsymbol{n}_{1r}^\dagger\right] = E\left[\boldsymbol{n}_{1i}\boldsymbol{n}_{1i}^\dagger\right] = E\left[\boldsymbol{n}_{2r}\boldsymbol{n}_{2r}^\dagger\right] = E\left[\boldsymbol{n}_{2i}\boldsymbol{n}_{2i}^\dagger\right] = \lambda\boldsymbol{\Sigma}, \\ &E\left[\boldsymbol{n}_{1kr}\boldsymbol{n}_{1kr}^\dagger\right] = E\left[\boldsymbol{n}_{1ki}\boldsymbol{n}_{1ki}^\dagger\right] = E\left[\boldsymbol{n}_{2kr}\boldsymbol{n}_{2kr}^\dagger\right] = E\left[\boldsymbol{n}_{2ki}\boldsymbol{n}_{2ki}^\dagger\right] = \boldsymbol{\Sigma}. \end{aligned} \tag{32}$$

With these definitions in mind, the rationale of the two-step design procedure is the following: first assume that $\boldsymbol{\Sigma}$ is known and derive decision rule according to a specific design criterion. Then, an adaptive detector is obtained by substituting $\boldsymbol{\Sigma}$ by the sample covariance matrix $\boldsymbol{S}$ [3].

Previous assumptions imply that the PDF of $\boldsymbol{Z}$ under H_l, $l = 0, 1$, is given by

$$f(\boldsymbol{Z};\boldsymbol{\Sigma},\lambda,l\alpha_r,l\alpha_i,H_l) = \frac{1}{(2\pi)^{2N}\det^2(\lambda\boldsymbol{\Sigma})}\exp\left\{-\frac{1}{2}\mathrm{Tr}\left[\frac{1}{\lambda}\boldsymbol{\Sigma}^{-1}\boldsymbol{W}_l(l\alpha_r,l\alpha_i)\right]\right\}, \quad (33)$$

where

$$\boldsymbol{W}_l(l\alpha_r,l\alpha_i) = (\boldsymbol{Z}_1 - l\alpha_r\boldsymbol{V})(\boldsymbol{Z}_1 - l\alpha_r\boldsymbol{V})^T + (\boldsymbol{Z}_2 - l\alpha_i\boldsymbol{V})(\boldsymbol{Z}_2 - l\alpha_i\boldsymbol{V})^T. \quad (34)$$

Under the assumption that $\boldsymbol{\Sigma}$ is known, the GLRT is given by

$$\frac{\max\limits_{\alpha_r,\alpha_i}\max\limits_{\lambda} f(\boldsymbol{Z};\boldsymbol{\Sigma},\lambda,\alpha_r,\alpha_i,H_1)}{\max\limits_{\lambda} f(\boldsymbol{Z};\boldsymbol{\Sigma},\lambda,0,0,H_1)} \underset{H_0}{\overset{H_1}{\gtrless}} \eta. \quad (35)$$

It is easy to show that the MLE of λ under H_l, $l=0,1$, is given by

$$\widehat{\lambda}_l = \frac{1}{4N}\mathrm{Tr}\left[\boldsymbol{\Sigma}^{-1}\boldsymbol{W}_l(l\alpha_r,l\alpha_i)\right]. \quad (36)$$

Substituting (33) and (36) in (35), after some algebraic manipulations, the natural logarithm of (35) can be recast as

$$\frac{\mathrm{Tr}\left(\boldsymbol{Z}_1^T\boldsymbol{\Sigma}^{-1}\boldsymbol{Z}_1 + \boldsymbol{Z}_2^T\boldsymbol{\Sigma}^{-1}\boldsymbol{Z}_2\right)}{\min\limits_{\alpha_r,\alpha_i} f(\alpha_r,\alpha_i)} \underset{H_0}{\overset{H_1}{\gtrless}} \eta, \quad (37)$$

where

$$f(\alpha_r,\alpha_i) = \mathrm{Tr}\Big[(\boldsymbol{Z}_1 - \alpha_r\boldsymbol{V})^T\boldsymbol{\Sigma}^{-1}(\boldsymbol{Z}_1 - \alpha_r\boldsymbol{V}) + (\boldsymbol{Z}_2 - \alpha_i\boldsymbol{V})^T\boldsymbol{\Sigma}^{-1}(\boldsymbol{Z}_2 - \alpha_i\boldsymbol{V})\Big]. \quad (38)$$

In the next step, our objective is to minimize $f(\alpha_r,\alpha_i)$ with respect to α_r and α_i. To this end, we evaluate the derivatives with respect to α_r and α_i, which are given by

$$\frac{\partial f(\alpha_r,\alpha_i)}{\partial\alpha_r} = -2\mathrm{Tr}\left[\boldsymbol{V}^T\boldsymbol{\Sigma}^{-1}(\boldsymbol{Z}_1 - \alpha_r\boldsymbol{V})\right],$$
$$\frac{\partial f(\alpha_r,\alpha_i)}{\partial\alpha_i} = -2\mathrm{Tr}\left[\boldsymbol{V}^T\boldsymbol{\Sigma}^{-1}(\boldsymbol{Z}_2 - \alpha_i\boldsymbol{V})\right]. \quad (39)$$

Setting to zero the two derivatives of (39), yields

$$\widehat{\alpha}_r = \frac{\mathrm{Tr}\left(\boldsymbol{V}^T\boldsymbol{\Sigma}^{-1}\boldsymbol{Z}_1\right)}{\mathrm{Tr}\left(\boldsymbol{V}^T\boldsymbol{\Sigma}^{-1}\boldsymbol{V}\right)},\ \widehat{\alpha}_i = \frac{\mathrm{Tr}\left(\boldsymbol{V}^T\boldsymbol{\Sigma}^{-1}\boldsymbol{Z}_2\right)}{\mathrm{Tr}\left(\boldsymbol{V}^T\boldsymbol{\Sigma}^{-1}\boldsymbol{V}\right)}. \quad (40)$$

Based on the above results, the GLRT can be recast as

$$\frac{\mathrm{Tr}^2\left(\boldsymbol{V}^T\boldsymbol{\Sigma}^{-1}\boldsymbol{Z}_1\right) + \mathrm{Tr}^2\left(\boldsymbol{V}^T\boldsymbol{\Sigma}^{-1}\boldsymbol{Z}_2\right)}{\mathrm{Tr}\left(\boldsymbol{V}^T\boldsymbol{\Sigma}^{-1}\boldsymbol{V}\right)\mathrm{Tr}\left(\boldsymbol{Z}^T\boldsymbol{\Sigma}^{-1}\boldsymbol{Z}\right)} \underset{H_0}{\overset{H_1}{\gtrless}} \eta. \quad (41)$$

Plugging $\boldsymbol{S}$ in place of $\boldsymbol{\Sigma}$ into (41), the GLRT is finally given by

$$\frac{\mathrm{Tr}^2\left(\boldsymbol{V}^T\boldsymbol{S}^{-1}\boldsymbol{Z}_1\right) + \mathrm{Tr}^2\left(\boldsymbol{V}^T\boldsymbol{S}^{-1}\boldsymbol{Z}_2\right)}{\mathrm{Tr}\left(\boldsymbol{V}^T\boldsymbol{S}^{-1}\boldsymbol{V}\right)\mathrm{Tr}\left(\boldsymbol{Z}^T\boldsymbol{S}^{-1}\boldsymbol{Z}\right)} \underset{H_0}{\overset{H_1}{\gtrless}} \eta. \quad (42)$$

In the sequel, we refer to detector (42) as the persymmetric and symmetric spectrum two-step GLRT for PHE (PSS-2SGLRT-PHE).

4. Performance assessment

In this section, we present some numerical examples to show the performances of the PSS-RAO-PHE and the PSS-2SGLRT-PHE in terms of probability of detection (P_d). To this end, we not only compare our detectors to the symmetric spectrum detectors that neglect the persymmetry, namely the so-called SS-ACE introduced in [35], but also compare the new receivers with the state-of-the-art persymmetric detectors that ignore the symmetric spectrum, including the persymmetric GLRT for PHE (P-GLRT-PHE) [29], the persymmetric RAO for PHE (P-RAO-PHE) [30], and the persymmetric adaptive coherence estimator (P-ACE) [27]. In the examples, we also include the ACE for known $\overline{\boldsymbol{M}}$, which cannot be used in practice but offers a baseline for comparison. This detector is referred to in the sequel as the optimum ACE (OPT-ACE), whose statistic is given by

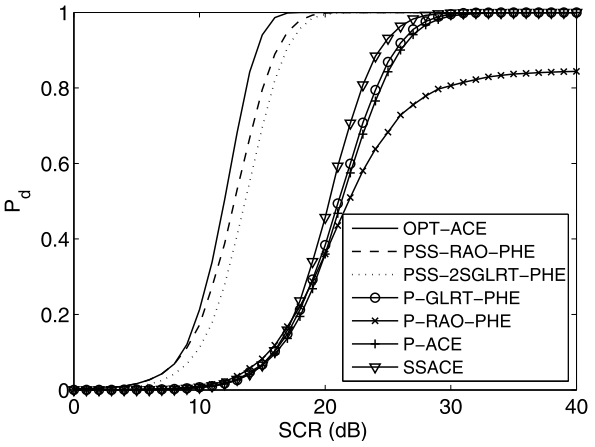

Fig. 1. P_d versus SCR for the OPT-ACE, PSS-RAO-PHE, PSS-2SGLRT-PHE, P-GLRT-PHE, P-RAO-PHE, P-ACE, and SS-ACE assuming $N=9$, $K=7$, $\gamma=3$, $\nu_d=0.3$, and CNR = 60 dB.

$$t_{\text{OPT-ACE}} = \frac{\left|\boldsymbol{v}^\dagger\overline{\boldsymbol{M}}^{-1}\boldsymbol{r}_0\right|^2}{(\boldsymbol{v}^\dagger\overline{\boldsymbol{M}}^{-1}\boldsymbol{v})(\boldsymbol{r}_0^\dagger\overline{\boldsymbol{M}}^{-1}\boldsymbol{r}_0)}. \quad (43)$$

The analysis is conducted both on simulated and real recorded data.

4.1. Numerical examples on simulated data

Since closed form expressions for P_d and P_{fa} are not available, we make use of standard Monte Carlo counting techniques and evaluate the thresholds necessary to ensure a preassigned value of P_{fa} resorting to $100/P_{fa}$ independent trials, while P_d values are estimated over 10^4 independent trials. All the examples assume $P_{fa}=10^{-4}$. We consider a clutter-dominated environment with the covariance matrix $\overline{\boldsymbol{M}} = \sigma_n^2\boldsymbol{I}_N + \sigma_c^2\boldsymbol{M}_c$, where $\sigma_n^2=1$ is the thermal noise power, $\sigma_c^2>0$ is the clutter power which is evaluated according to a given clutter-to-noise ratio (CNR) defined as $\mathrm{CNR}=\sigma_c^2/\sigma_n^2$. As to $\boldsymbol{M}_c$, it is Gaussian shaped with one-lag correlation coefficient ρ, which means that the (i,j)th element of $\boldsymbol{M}_c$ is $\rho^{|i-j|^2}$. The signal-to-clutter ratio (SCR) is defined as $\mathrm{SCR}=|\alpha|^2\boldsymbol{v}(\nu_d)^\dagger\overline{\boldsymbol{M}}^{-1}\boldsymbol{v}(\nu_d)$, where the temporal steering vector $\boldsymbol{v}(\nu_d)$ is given by $\boldsymbol{v}(\nu_d) = \frac{1}{\sqrt{N}}\left[e^{-j2\pi\frac{N-1}{2}\nu_d}\ldots 1\ldots e^{j2\pi\frac{N-1}{2}\nu_d}\right]$ with the normalized Doppler frequency $\nu_d=0.3$. Finally, all numerical examples assume $P_{fa}=10^{-4}$ and $\rho=0.9$.

In Fig. 1, we plot the P_d versus the SCR for the considered detectors assuming $N=9$, $K=7$, $\gamma=3$, and CNR = 60 dB. The figure shows that the PSS-RAO-PHE and the PSS-2SGLRT-PHE significantly outperform the traditional state-of-the-art counterparts which either ignore the persymmetry or the symmetric spectrum. Precisely, the best detection performance is ensured by the PSS-RAO-PHE with a gain of about 0.7 dB at $P_d=0.9$ over the PSS-2SGLRT-PHE. Such a gain increases to above 8.1 dB with respect to persymmetric detectors and the SS-ACE. Thus, joint exploitation of the clutter and system symmetry properties is a very effective means to improve performance in the presence of a small number of secondary data. However, the above-mentioned P_d gain can be reduced by increasing K, due to the fact that the estimate of $\overline{\boldsymbol{M}}$ becomes more

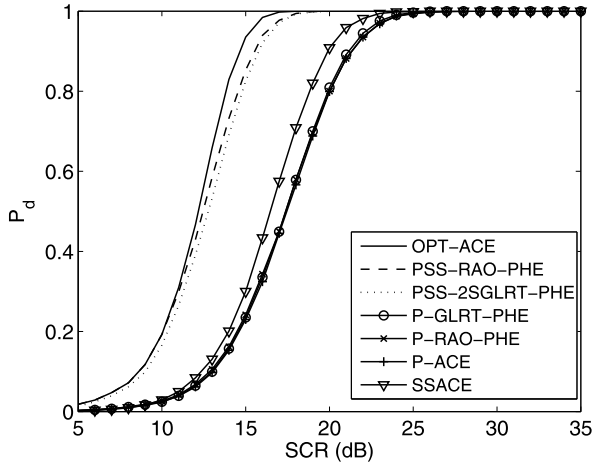

Fig. 2. $P_{\rm d}$ versus SCR for the OPT-ACE, PSS-RAO-PHE, PSS-2SGLRT-PHE, P-GLRT-PHE, P-RAO-PHE, P-ACE, and SS-ACE assuming $N = 9$, $K = 9$, $\gamma = 3$, $\nu_d = 0.3$, and CNR = 60 dB.

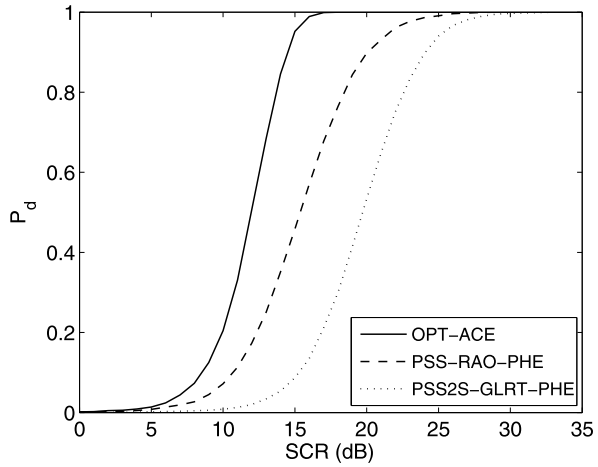

Fig. 3. $P_{\rm d}$ versus SCR for the OPT-ACE, PSS-RAO-PHE, PSS-2SGLRT-PHE, assuming $N = 9$, $K = 4$, $\gamma = 3$, $f_d = 0.3$, and CNR = 60 dB.

reliable, as shown in Fig. 2, where we plot the P_d of the considered detectors assuming the same system parameters as Fig. 1, but for $K = 9$. Note also that the SS-ACE guarantees better performance than the considered three persymmetric detectors.

In Fig. 3, we consider a very training-limited scenario, namely, $N = 9$, and $K = 4$. In this case, only the newly proposed detectors are involved, due to the fact that they can work under the constraint $K < N/2$. Inspection of the figure shows that the PSS-RAO-PHE ensures better detection performance than the PSS-2SGLRT-PHE. Precisely, the performance gain with respect to the PSS-2SGLRT-PHE is about 4.0 dB at $P_d = 0.9$.

4.2. Numerical examples on real data

The aim of this section is to study the behavior of the newly proposed detectors in the presence of live clutter data. To this end, we exploit the MIT-LL Phase-One radar dataset, which is observed by a stationary monostatic radar, contains land clutter and refers to different bands, polarizations, range resolutions, and scanning modes. In [45], it is shown that the real data exhibits a symmetric Power Spectral Density (PSD) centered around the zero-Doppler frequency. Moreover, its persymmetric property has been corroborated in [33].

Each data file is composed of N_t temporal returns from N_s range cells which are stored in an $N_t \times N_s$ complex matrix. The most important parameters of the L-Band clutter datasets, are reported in Table 1. We highlight that the considered area contains windblown vegetation primary composed of mixed deciduous trees and occasional pine and cedar. At the time of the experiment the deciduous trees did not yet have their leaves. Further details on the description of the dataset can be found in [46, and references therein], where is possible to observe that the spectrum of the clutter live data satisfy the assumption to by symmetrical (as could be expected from terrain clutter) while the power level versus the range cell is non-homogeneous.

Table 1
Specifications of the land clutter dataset.

	Dataset H067038 3.iq and H067037 2.iq
Date	May 3, 1985
Number of pulses N_t	30720
Number of cells N_s	76
Polarizations	HH and VV
RF frequency	1.23 GHz
Pulse length	100 ns
Pulse repetition frequency	500 Hz
Radar scan mode	Fixed azimuth
Radar azimuth angle	235
Grazing angles	0.86 to 0.54 deg
Range	2000–3125 m
Radar beam width	3.4 deg
Range resolution	15 m
Quantization bit	13
Mean/Max wind speed	27/34 km/h (HH) 32/32 km/h (VV)

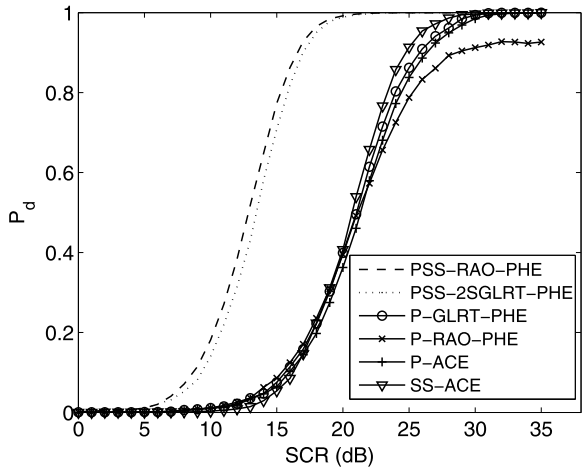

Fig. 4. $P_{\rm d}$ versus SCR for the PSS-RAO-PHE, PSS-2SGLRT-PHE, P-GLRT-PHE, P-RAO-PHE, P-ACE, and SS-ACE assuming $N = 9$, $K = 7$, $\nu_d = 0.3$, real data, vertical polarization.

The detection performance analysis is conducted in accordance to the procedure shown in [34]. The P_d of the receivers is evaluated comparing the statistic over the cell under test with the threshold provided by the procedure of [34]. As to the temporal steering vector, ν_d is chosen equal to 0.3. Several cells under test have been tried over the entire dataset, leading to very similar results. In the following, the results for the cell under test number 25 are reported.

The P_d curves versus the SCR are shown in Figs. 4, 5, and 6. Precisely, in Fig. 4 the performances of all the analyzed receivers are reported for $N = 9$, $K = 7$ and $P_{fa} = 10^{-4}$, showing very similar results with respect to the simulated data; the proposed receivers exhibit the best performances under the assumption of limited training data. Also in Fig. 5, the behavior experimented for the simulated data is observed, with the proposed receivers outperforming the others receivers of 4.5 dB for a reference $P_d = 0.9$. Finally in Fig. 6, the results for the very stressing scenarios, i.e.,

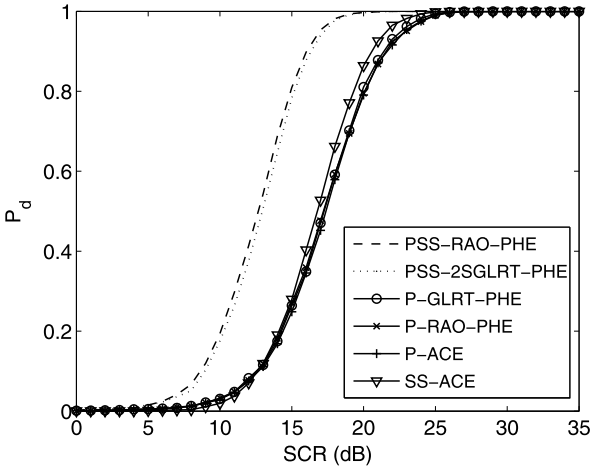

Fig. 5. $P_{\rm d}$ versus SCR for the PSS-RAO-PHE, PSS-2SGLRT-PHE, P-GLRT-PHE, P-RAO-PHE, P-ACE, and SS-ACE assuming $N = 9$, $K = 9$, $\nu_d = 0.3$, real data, vertical polarization.

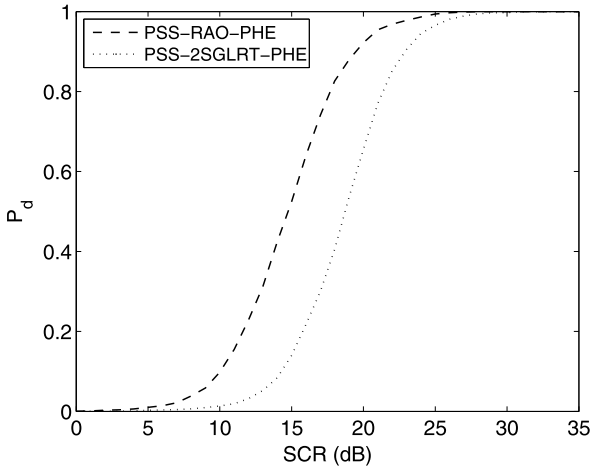

Fig. 6. $P_{\rm d}$ versus SCR for the PSS-RAO-PHE, PSS-2SGLRT-PHE, assuming $N = 9$, $K = 4$, $\nu_d = 0.3$, real data, vertical polarization.

$N = 9$, $K = 4$ and $P_{fa} = 10^{-4}$, are reported. The figure highlights that the PSS-RAO-PHE and the PSS-2SGLRT-PHE obtain satisfactory performances and can be used in real environments under very severe conditions of very limited amount of training data. Meanwhile, the PSS-RAO-PHE guarantees better detection performance than the PSS-2SGLRT-PHE. All these analyses have been repeated also for the HH polarization (not reported here for the sake of brevity) and confirm the trend observed for the VV polarization.

As a final remark, we would like to highlight that if the clutter and system symmetry properties are violated due to amplitude and phase errors caused by the practical nature of real hardware, the performance of the proposed detectors will be degraded. A sensitivity analysis can highlight these aspects, although a thorough performance analysis is out of the scope of this work.

5. Conclusions

In this paper, we have considered the problem of adaptive detection of a point-like target buried in partially homogeneous Gaussian clutter. For the sake of deriving these new detectors, we jointly exploit the persymmetric structure of the CCM as well as the symmetry in the clutter spectral characteristics. As first step toward detector designs, we transfer the data test problem from the complex to the real domain by two consecutive transformations, then we resort to the Rao test and the two-step modifications of the GLRT. The performance assessment has demonstrated that the proposed receivers can significantly outperform its natural competitors which either ignore the persymmetry or the symmetric spectrum. Possible future research could involve the extension of the proposed framework to detect distributed targets [33,47,48] or operate under non-Gaussian clutter [49–51].

Acknowledgments

This work was supported by the National Natural Science Foundation of China under Grant No. 61571434.

References

[1] A. De Maio, M. Greco, Modern Radar Detection Theory, IET Scitech Publishing, 2015.
[2] E.J. Kelly, An adaptive detection algorithm, IEEE Trans. Aerosp. Electron. Syst. 2 (1986) 115–127.
[3] F.C. Robey, D.R. Fuhrmann, E.J. Kelly, R. Nitzberg, A CFAR adaptive matched filter detector, IEEE Trans. Aerosp. Electron. Syst. 28 (1) (1992) 208–216.
[4] A. De Maio, A new derivation of the adaptive matched filter, IEEE Signal Process. Lett. 11 (10) (2004) 792–793.
[5] A. De Maio, Rao test for adaptive detection in Gaussian interference with unknown covariance matrix, IEEE Trans. Signal Process. 55 (7) (2007) 3577–3584.
[6] F. Bandiera, D. Orlando, G. Ricci, Advanced Radar Detection Schemes Under Mismatched Signal Models, 2009, San Rafael, US.
[7] W. Liu, W. Xie, Y. Wang, Parametric detector in the situation of mismatched signals, IET Radar Sonar Navig. 8 (1) (2014) 48–53.
[8] W. Liu, W. Xie, J. Liu, Y. Wang, Adaptive double subspace signal detection in Gaussian background. Part I: homogeneous environments, IEEE Trans. Signal Process. 62 (9) (2014) 2345–2357.
[9] D. Orlando, G. Ricci, A Rao test with enhanced selectivity properties in homogeneous scenarios, IEEE Trans. Signal Process. 58 (10) (2010) 5385–5390.
[10] N.B. Pulsone, C.M. Rader, Adaptive beamformer orthogonal rejection test, IEEE Trans. Signal Process. 49 (3) (2001) 521–529.
[11] I.S. Reed, J.D. Mallett, L.E. Brennan, Rapid convergence rate in adaptive arrays, IEEE Trans. Aerosp. Electron. Syst. 10 (6) (1974) 853–863.
[12] S. Haykin, Adaptive Filter Theory, 4th ed., 2002.
[13] M.C. Wicks, M. Rangaswamy, R. Adve, B. Hale, Space-time adaptive processing: a knowledge-based perspective for airborne radar, IEEE Trans. Signal Process. (2006) 51–65.
[14] W.L. Melvin, Space-time adaptive radar performance in heterogeneous clutter, IEEE Trans. Aerosp. Electron. Syst. 36 (2) (2000) 621–633.
[15] A. Aubry, V. Carotenuto, A. De Maio, G. Foglia, Exploiting multiple a priori spectral models for adaptive radar detection, IET Radar Sonar Navig. 8 (7) (2014) 695–707.
[16] E. Conte, A. De Maio, A. Farina, G. Foglia, Design and analysis of a knowledge-aided radar detector for Doppler processing, IEEE Trans. Aerosp. Electron. Syst. 42 (3) (2006) 1058–1079.
[17] A. Aubry, Demonstration of knowledge aided STAP using measured airborne data, IEE Proc. Radar Sonar Navig. 153 (6) (2006) 487–494.
[18] A. De Maio, A. Farina, G. Foglia, Knowledge-based recursive least squares techniques for heterogeneous clutter suppression, IET Radar Sonar Navig. 1 (2) (2007) 106–115.
[19] L. Landi, A. De Maio, S. De Nicola, A. Farina, Knowledge-aided covariance matrix estimation: a MAXDET approach, IET Radar Sonar Navig. 3 (4) (2009) 341–356.
[20] A. Aubry, A. De Maio, L. Pallotta, A. Farina, Maximum likelihood estimation of a structured covariance matrix with a condition number constraint, IEEE Trans. Signal Process. 60 (6) (2012) 3004–3021.
[21] R. Nitzberg, Application of maximum likelihood estimation of persymmetric covariance matrices to adaptive processing, IEEE Trans. Aerosp. Electron. Syst. 16 (1) (1980) 124–127.
[22] R. Klemm, Principles of Space-Time Adaptive Processing, 2002.
[23] P. Wang, Z. Sahinoglu, M. Pun, H. Li, Persymmetric parametric adaptive matched filter for multichannel adaptive signal detection, IEEE Trans. Signal Process. 60 (6) (2012) 3322–3328.
[24] L. Cai, H. Wang, A persymmetric multiband GLR algorithm, IEEE Trans. Aerosp. Electron. Syst. 28 (3) (1992) 806–816.
[25] G. Pailloux, P. Forster, J.P. Ovarlez, F. Pascal, Persymmetric adaptive radar detectors, IEEE Trans. Aerosp. Electron. Syst. 47 (4) (2011) 2376–2390.
[26] C. Hao, S. Gazor, G. Foglia, B. Liu, H. C., Persymmetric adaptive detection and range estimation of a small target, IEEE Trans. Aerosp. Electron. Syst. 51 (4) (2015) 2590–2604.
[27] Y. Gao, G. Liao, S. Zhu, X. Zhang, D. Yang, Persymmetric adaptive detectors in homogeneous and partially homogeneous environments, IEEE Trans. Signal Process. 62 (2) (2014) 331–342.

[28] S.U. Pillai, Y.L. Kim, J.R. Guerci, Generalized forward/backward subaperture smoothing techniques for sample starved STAP, IEEE Trans. Signal Process. 48 (12) (2000) 3569–3574.
[29] M. Casillo, A. De Maio, S. Iommelli, L. Landi, A persymmetric GLRT for adaptive detection in partially-homogeneous environment, IEEE Signal Process. Lett. 14 (12) (2007) 1016–1019.
[30] C. Hao, D. Orlando, X. Ma, C. Hou, Persymmetric Rao and Wald tests for partially homogeneous environment, IEEE Signal Process. Lett. 19 (9) (2012) 587–590.
[31] J. Liu, H. Li, B. Himed, Persymmetric adaptive target detection with distributed MIMO radar, IEEE Trans. Aerosp. Electron. Syst. 51 (1) (2015) 372–382.
[32] J. Liu, G. Cui, H. Li, B. Himed, On the performance of a persymmetric adaptive matched filter, IEEE Trans. Aerosp. Electron. Syst. 51 (4) (2015) 2605–2614.
[33] C. Hao, D. Orlando, G. Fogliab, X. Ma, S. Yan, C. Hou, Persymmetric adaptive detection of distributed targets in partially-homogeneous environment, Digit. Signal Process. 24 (1) (2014) 42–51.
[34] A. De Maio, D. Orlando, C. Hao, G. Foglia, Adaptive detection of point-like targets in spectrally symmetric interference, IEEE Trans. Signal Process. 64 (12) (2016) 3207–3220.
[35] C. Hao, D. Orlando, A. Farina, S. Iommelli, C. Hou, Symmetric spectrum detection in the presence of partially homogeneous environment, in: 2016 IEEE Radar Conference, RadarConf, IEEE, 2016, pp. 1–4.
[36] C. Hao, D. Orlando, G. Foglia, G. Giunta, Knowledge-based adaptive detection: Joint exploitation of clutter and system symmetry properties, IEEE Signal Process. Lett. 23 (10) (2016) 1489–1493.
[37] S. Kraut, L.L. Scharf, The CFAR adaptive subspace detector is a scale-invariant GLRT, IEEE Trans. Signal Process. 47 (9) (1999) 2538–2541.
[38] C. Hao, D. Orlando, G. Foglia, X. Ma, C. Hou, Adaptive radar detection and range estimation with oversampled data for partially homogeneous environment, IEEE Signal Process. Lett. 22 (9) (2015) 1359–1363.
[39] A. De Maio, C. Hao, D. Orlando, An adaptive detector with range estimation capabilities for partially homogeneous environment, IEEE Signal Process. Lett. 21 (3) (2014) 325–329.
[40] W. Liu, W. Xie, J. Liu, Y. Wang, Adaptive double subspace signal detection in Gaussian background. Part II: partially homogeneous environments, IEEE Trans. Signal Process. 62 (9) (2014) 2358–2369.
[41] E. Conte, A. De Maio, An invariant framework for adaptive detection in partially homogeneous environment, WSEAS Trans. Circuits 2 (1) (2003) 282–287.
[42] A. Ghobadzadeh, S. Gazor, A. Taban, S.M. Moshtaghioun, Invariance and optimality of CFAR detectors in binary composite hypothesis tests, IEEE Trans. Signal Process. 62 (14) (2014) 3523–3535.
[43] S.M. Kay, Fundamentals of Statistical Signal Processing: Detection Theory, vol. 2, 1998.
[44] E. Conte, A. De Maio, G. Ricci, GLRT-based adaptive detection algorithms for range-spread targets, IEEE Trans. Signal Process. 49 (7) (2001) 1336–1348.
[45] J.B. Billingsley, A. Farina, F. Gini, M.S. Greco, L. Verrazzani, Statistical analyses of measured radar ground clutter data, IEEE Trans. Aerosp. Electron. Syst. 35 (2) (1999) 579–593.
[46] A. De Maio, G. Foglia, E. Conte, A. Farina, CFAR behavior of adaptive detectors: an experimental analysis, IEEE Trans. Aerosp. Electron. Syst. 41 (1) (2005) 233–251.
[47] K. Gerlach, M.J. Steiner, Adaptive detection of range distributed targets, IEEE Trans. Signal Process. 47 (7) (1999) 1844–1851.
[48] F. Bandiera, A. De Maio, A.S. Greco, G. Ricci, Adaptive radar detection of distributed targets in homogeneous and partially homogeneous noise plus subspace interference, IEEE Trans. Signal Process. 55 (4) (2007) 1223–1237.
[49] S. Watts, Radar detection prediction in k-distributed sea clutter and thermal noise, IEEE Trans. Aerosp. Electron. Syst. 23 (1) (1987) 40–45.
[50] M. Rangaswamy, Statistical analysis of the nonhomogeneity detector for non-Gaussian interference backgrounds, IEEE Trans. Signal Process. 53 (6) (2005) 2101–2111.
[51] K.J. Sangston, F. Gini, M. Greco, Coherent radar target detection in heavy-tailed compound-Gaussian clutter, IEEE Trans. Aerosp. Electron. Syst. 48 (1) (2012) 64–77.

Goffredo Foglia was born in San Paolo Belsito, Italy, on November 20, 1977. He received the Dr. Eng. degree in June 2003 from the University of Naples Federico II, and the Ph.D. degree in information engineering in February 2007 from the University of Cassino, Italy. In February 2004 he joined Elettronica S.p.A., Rome, Italy. Today he is responsible for the Integrated Electronic Warfare System, with special emphasis on the electronic support measure functionalities, in the Research and Advanced Systems Design Department. His current research lies in the field of radar applications, EW system architectures and algorithms.

Chengpeng Hao received the B.S. and the M.S. degrees in electronic engineering from Beijing Broadcasting Institute, Beijing, China, in 1998 and 2001 respectively. He received the Ph.D. degree in signal and information processing from Institute of Acoustics, Chinese Academy of Sciences, Beijing, China, in 2004. He is currently a Professor of the State Key Laboratory of Information Technology for Autonomous Underwater vehicles, Chinese Academy of Sciences. His research interests are in the field of statistical signal processing with more emphasis on adaptive sonar and radar signal processing. He is Senior Member of IEEE. He served as a Guest Editor for the EURASIP Journal on Advances in Signal Processing for the issue on "Advanced Techniques for Radar Signal Processing".

Gaetano Giunta received the Dr. Eng. degree in electronic engineering from the University of Pisa, Pisa, Italy, in 1985, and the Ph.D. degree in information and communication engineering from the University of Rome "La Sapienza", Rome, Italy. Currently, he is a Full Professor of Telecommunications with the Department of Engineering at the University of Roma Tre. The research interests of Prof. Giunta are in signal and image processing for mobile communications and wireless systems. He is a member of national and international research groups and the local responsible of projects on signal processing techniques in wireless and mobile systems. Since 1988, he has been a member (Senior Member since 2011) of the IEEE Signal Processing, Communications, and Vehicular Technology Societies. In particular, he has served as a reviewer for several IEEE and IET scientific journals.

Danilo Orlando was born in Gagliano del Capo, Italy, on August 9, 1978. He received the Dr. Eng. degree (with honors) in computer engineering and the Ph.D. degree (with maximum score) in information engineering, both from the University of Salento (formerly University of Lecce), Italy, in 2004 and 2008, respectively. From September 2011 to April 2015, he has worked at Elettronica S.p.A. engaged as system analyst in the field of Electronic Warfare. In May 2015, he joined Università degli Studi "Niccolò Cusano", where he is currently Associate Professor. His main research interests are in the field of statistical signal processing and image processing with more emphasis on adaptive detection and tracking of multiple targets in multisensor scenarios. He is Senior Member of IEEE and author or co-author of more than 70 scientific publications in international journals, conferences, and books.